THE EFFECTS OF SOIL–STRUCTURE INTERACTION MODELING TECHNIQUES ON IN-STRUCTURE RESPONSE SPECTRA

J. J. JOHNSON, D. A. WESLEY, I. T. ALMAJAN

General Atomic Company,
San Diego, P.O. Box 81608, California 92138, U.S.A.

SUMMARY

The seismic design of nuclear power plant components is normally based on in-structure response spectra generated from an overall plant analysis which accounts for soil-structure interaction. For preliminary design, it is desirable to consider a broad range of site conditions which requires an economical analysis of the soil-structure interaction phenomenon. The purpose of this paper is to compare the results obtained from a simplified approach utilizing stiffness proportional composite damping with those obtained utilizing more refined representations of the soil-structure interaction phenomenon. Thereby, the limits of applicability of the simplified approach are determined.

The structure considered for this investigation consisted of the reactor containment building (RCB) and prestressed concrete reactor vessel (PCRV) for a HTGR plant. A conventional lumped-mass dynamic model in three dimensions was used in the study. The horizontal and vertical response, which are uncoupled due to the symmetry of the structure, were determined for horizontal and vertical excitation. Five different site conditions ranging from competent rock to a soft soil site were considered.

The simplified approach to the overall plant analysis utilized stiffness proportional composite damping with a limited amount of soil damping consistent with US NRC regulatory guidelines. Selected cases were also analyzed assuming a soil damping value approximating the theoretical value. The results from the simplified approach were compared to those determined by rigorously coupling the structure to a frequency independent half-space representation of the soil. Finally, equivalent modal damping ratios were found by matching the frequency response at a point within the coupled soil-structure system determined by solution of the coupled and uncoupled equations of motion.

The basis for comparison of the aforementioned techniques was the response spectra at selected locations within the soil-structure system. Each of the five site conditions was analyzed and in-structure response spectra were generated. The response spectra were combined to form a design envelope which encompasses the entire range of site parameters. Both the design envelopes and the site-by-site results were compared.

The results of this investigation led to separate conclusions concerning the applicability of the simplified approach to the determination of the soil-structure system depending on whether response was in the horizontal or vertical direction. The in-structure response spectra in the horizontal direction compared on a site-by-site basis and as a design envelope showed only minor deviations due to the analysis technique applied. However, the in-structure response spectra in the vertical direction as determined by the simplified approach were significantly higher than those found by utilizing a more refined representation of the soil-structure interaction phenomenon. Further, the response spectra from the simplified approach exhibited highly pronounced peaks whereas the response spectra from more refined analyses were of a broad band nature. In conclusion, a simplified approach to the computation of the in-structure response spectra for horizontal excitations was shown to be valid. However, its application to the computation of the vertical response is unnecessarily conservative.

1. Introduction

The seismic design of nuclear power plant components is normally based on in-structure response spectra generated from an overall plant analysis which accounts for soil-structure interaction. For preliminary design, it is desirable to consider a broad range of site conditions which requires an economical analysis of the soil-structure interaction phenomenon. The purpose of this paper is to compare the results obtained from a simplified approach utilizing stiffness proportional composite damping with those obtained utilizing more refined representations of the soil-structure interaction phenomenon. Thereby, the limits of applicability of the simplified approach are determined.

The structure considered for this investigation consists of the reactor containment building (RCB) and prestressed concrete reactor vessel (PCRV) for an HTGR. A conventional lumped-mass dynamic model in three-dimensions is used in the study. The horizontal and vertical response, which are uncoupled due to the symmetry of the structure, are determined for horizontal and vertical excitations. Five different site conditions ranging from competent rock to a soft soil site are considered.

The results which form the basis of comparison are determined by rigorously coupling the structure to a frequency independent half-space representation of the soil. This precludes the consideration of rapidly varying soil properties such as layering of soils. The embedment of the structure to a significant depth is not considered. The simplified approach considered herein utilizes stiffness proportional composite damping with a limited amount of soil damping consistent with US NRC regulatory guidelines. More refined techniques of determining equivalent modal damping ratios are examined. Damping ratios defined by matching the frequency response at a point within the coupled soil-structure system as determined by solution of the coupled and uncoupled equations of motion are investigated. Further, the proportioning of the damping characteristics according to the energy dissipated in each member is considered.

The basis for comparison of the aforementioned techniques is the response spectra at selected locations within the soil-structure system. Each of the five site conditions is analyzed and in-structure response spectra generated. The response spectra are combined to form a design envelope which encompasses the entire range of site parameters. Both the design envelopes and the site-by-site results are compared.

In the HTGR, the reactor containment building (RCB) and the prestressed concrete reactor vessel (PCRV) are supported on a common base slab as depicted in Figure 1. The reactor containment building is a cylindrical, prestressed concrete structure with a dome roof of elliptical shape. The prestressed concrete reactor vessel is a multi-cavity vessel housing the reactor internals. The overall dimensions of the RCB/PCRV configuration are depicted in Fig. 1. A simplified dynamic mathematical model of the RCB/PCRV configuration consisting of a conventional lumped-mass structure supported by a rigid base slab is utilized. A schematic view of the model is superposed on the structure in Fig. 1. The model is a general three-dimensional representation. However, the resulting motion is uncoupled in the two horizontal and vertical directions due to the symmetry of the structure. The damping associated with the structure is taken to be two percent of critical for all fixed base modes of vibration.

All analyses reported herein were performed using artificial earthquake time histories as input for the horizontal and vertical ground motions. The artificial earthquakes have response spectra which envelope the design response spectra as given in the US NRC Regulatory Guide 1.60 [1]. The results presented herein are due to a peak horizontal ground acceleration of 1.0 g and may be scaled linearly to any other acceleration level.

The analyses have been performed for five different soil conditions. The subsurface conditions are assumed to be uniform with depth permitting an elastic half space representation of the supporting medium. A set of soil properties which are representative of each site are tabulated in Table I.

2. Soil-Structure Interaction

2.1 Equations of Motion

The equations of motion of the coupled soil-structure system are derived herein. The treatment presented follows the basic approach of Tsai [2] although extended to permit general three-dimensional motion [3,4]. In the present analysis, relative deformation of the base mat is not permitted, i.e., the base mat is assumed to be rigid. This does not limit the applicability of the approach, and is a reasonable assumption for the structure being studied. In subsequent discussions, the term super-structure refers to the fixed-base structure. This connotation is convenient because the dynamic characteristics of the structure are represented by the fixed-base structural eigensystem and damping ratios.

The deformation of a typical node i of the super-structure relative to the base is denoted $\{X\}_i$ where $\{X\}_i$ is the partitioned vector:

$$\{X\}_i = \begin{Bmatrix} X_i \\ \hline \theta_i \end{Bmatrix} = \langle\, u \;\; v \;\; w \;\vdots\; \theta_x \;\; \theta_y \;\; \theta_z \,\rangle^T \tag{1}$$

The quantities (u, v, w, θ_x, θ_y, θ_z) are respectively the displacements in the (x, y, z) directions and the rotations about the (x, y, z) axes. In similar notation, the deformation of the base mat relative to the ground is given by $\{X\}_b$. Hence, the deformation of node point i relative to the ground, $\{Y\}_i$, is given by:

$$\begin{Bmatrix} Y_i \\ \hline \phi_i \end{Bmatrix} = \begin{Bmatrix} X_i \\ \hline \theta_i \end{Bmatrix} + \begin{bmatrix} [I] & [\lambda_i] \\ \hline 0 & [I] \end{bmatrix} \begin{Bmatrix} X_b \\ \hline \theta_b \end{Bmatrix} \tag{2}$$

$$\text{where} \quad [\lambda_i] = \begin{bmatrix} 0 & (z_i - z_b) & -(y_i - y_b) \\ -(z_i - z_b) & 0 & (x_i - x_b) \\ (y_i - y_b) & (x_i - x_b) & 0 \end{bmatrix} \tag{3}$$

and $[I]$ is the identity matrix.

The quantities (x_i, y_i, z_i) and (x_b, y_b, z_b) are the coordinates of node point i and the base, respectively. The coupled soil-structure system is excited by translational motions of the ground. The quantity $\{\ddot{u}\}_g$ denotes the excitation where

$$\{\ddot{u}\}_g = \begin{Bmatrix} \ddot{u} \\ \hline 0 \end{Bmatrix} = \langle\, u_x \;\; u_y \;\; u_z \;\vdots\; 0 \;\; 0 \;\; 0 \,\rangle^T \tag{4}$$

Further, the partitioned vector $\{\ddot{U}\}$ represents a vector of length equal to the number of super-structure degrees of freedom with a value of ($\ddot{u}_x$, $\ddot{u}_y$, $\ddot{u}_z$) corresponding to each super-structure degree-of-freedom in the (x, y, z) directions, respectively, and a zero for each rotational degree-of-freedom.

The equations of motion for the coupled soil-structure system are:

$$[M]\left(\{\ddot{Y}\} + \{\ddot{U}\}\right) + [C]\{\dot{X}\} + [K]\{X\} = 0 \tag{5}$$

$$[M_b]\left(\{\ddot{X}\}_b + \{\ddot{u}\}_g\right) + [C_b]\{\dot{X}\}_b + [K_b]\{X\}_b = -[H]^T[M]\left(\{\ddot{Y}\} + \{\ddot{U}\}\right) \tag{6}$$

The matrix equation eq. (5) represents the equations of motion for the super-structure degrees-of-freedom. In the most general three-dimensional case, the number of equations is six times the number of super-structure node points. In eq. (6), the term $[M_b]$ denotes the base mat mass matrix. The matrices $[K_b]$ and $[C_b]$ denote the stiffness and damping terms associated with the foundation. The matrix $[H]^T$ results from the super-structure's forces transferred to the base mat and is given by:

$$[H]^T = \left[\begin{array}{c|c|c|c|c|c|c} [I] & 0 & [I] & 0 & [I] & 0 & \cdots \\ \hline [\lambda_1]^T & [I] & [\lambda_2]^T & [I] & [\lambda_3]^T & [I] & \cdots \end{array}\right] \tag{7}$$

where $[\lambda_i]$ has been defined previously. Rearranging and consolidating eqs. (5) and (6) yields eq. (8).

$$\left[\begin{array}{c|c} M & 0 \\ \hline 0 & M_b \end{array}\right]\{\ddot{v}\} + \left[\begin{array}{c|c} C & -CH \\ \hline -H^TC & C_b + H^TCH \end{array}\right]\{\dot{v}\} + \left[\begin{array}{c|c} K & -KH \\ \hline -H^TK & K_b + H^TKH \end{array}\right]\{v\} = -\left[\begin{array}{c|c} M & 0 \\ \hline 0 & M_b \end{array}\right]\left\{\begin{array}{c} \ddot{u} \\ \ddot{u}_g \end{array}\right\} \tag{8}$$

where $\{v\} = \left\{\begin{array}{c} Y \\ \hline X_b \end{array}\right\}$.

In this approach, it is convenient to represent the super-structure dynamic characteristics by the fixed-base eigensystem and damping ratios. To do so requires the existence of classical normal modes for the damped system. In general, damped systems do not possess classical normal modes and the homogeneous solution of the equations of motion leads to complex mode shapes. Herein, for the lightly damped super-structure, the normal modes of the damped system are approximated by the normal modes of the undamped system with identical stiffness and mass characteristics. Hence, the linear coordinate transformation:

$$\{Y\} = [\phi]\{q\} \tag{9}$$

when applied to the equation of motion for the super-structure:

$$[M]\{\ddot{Y}\} + [C]\{\dot{Y}\} + [K]\{Y\} = -[M]\{\ddot{U}\} \tag{10}$$

yields

$$\{\ddot{q}\} + [\,2\beta_j\omega_j\,]\{\dot{q}\} + [\,\omega_j^2\,]\{q\} = -\{\gamma_x\}\ddot{u}_x - \{\gamma_y\}\ddot{u}_y - \{\gamma_z\}\ddot{u}_z \tag{11}$$

The quantities ω_j and β_j are the undamped natural frequency and the fraction of critical damping of the j^{th} mode, respectively. The vector $\{\gamma_\ell\}$ is comprised of the modal participation factors γ_j for an excitation in the ℓ direction:

$$\{\gamma_\ell\} = \frac{[\phi]^T[M]\{\delta_\ell\}}{[\phi]^T[M][\phi]} \qquad \ell = x, y, z \tag{12}$$

The vector $\{\delta_\ell\}$ is a vector with a one for ℓ direction displacements and a zero for all others.

To simplify eq. (8), consider the linear coordinate transformation:

$$\{v\} = [A]\{r\} \tag{13}$$

where $$[A] = \left[\begin{array}{c|c} [\phi] & 0 \\ \hline 0 & [M_b]^{-1/2} \end{array}\right] \tag{14}$$

The columns of $[\phi]$ are composed of the super-structure eigenvectors $\{\phi_j\}$. The matrix $[M_b]^{-1/2}$ satisfies the relation:

$$\left([M_b]^{-1/2}\right)^T [M_b]\, [M_b]^{-1/2} = [I] \tag{15}$$

Substituting eq. (13) into eq. (8), premultiplying by the matrix $[A]^T$, and simplifying yields:

$$\{\ddot{r}\} + \left[\begin{array}{c|c} \lceil 2\beta_j\omega_j \rfloor & -\lceil 2\beta_j\omega_j \rfloor\, [\Gamma|\Lambda]\, [M_b]^{-1/2} \\ \hline -\left([M_b]^{-1/2}\right)^T [\Gamma|\Lambda]^T \lceil 2\beta_j\omega_j \rfloor & \left([M_b]^{-1/2}\right)^T\left([C_b] + [\Gamma|\Lambda]^T \lceil 2\beta_j\omega_j \rfloor\, [\Gamma|\Lambda]\right)[M_b]^{-1/2} \end{array}\right]\{\dot{r}\}$$

$$+\left[\begin{array}{c|c} \lceil \omega_j^2 \rfloor & -\lceil \omega_j^2 \rfloor\, [\Gamma|\Lambda]\, [M_b]^{-1/2} \\ \hline -\left([M_b]^{-1/2}\right)^T [\Gamma|\Lambda]^T \lceil \omega_j^2 \rfloor & \left([M_b]^{-1/2}\right)^T \left([K_b] + [\Gamma|\Lambda]^T \lceil \omega_j^2 \rfloor\, [\Gamma|\Lambda]\right)[M_b]^{-1/2} \end{array}\right]\{r\} = -\left[\begin{array}{c} [\Gamma|0] \\ \hline \left([M_b]^{-1/2}\right)^T [M_b] \end{array}\right]\{\ddot{u}\}_g \tag{16}$$

The matrices $[\Gamma]$ and $[\Lambda]$ for the general three-dimensional case are given by:

$$[\Gamma] = [\gamma_x|\gamma_y|\gamma_z] \qquad [\Lambda] = [\Lambda_x|\Lambda_y|\Lambda_z] = [\phi]^T\, [M] \begin{bmatrix} \lambda_1 \\ I \\ \lambda_2 \\ I \\ \vdots \end{bmatrix} \tag{17}$$

Hence, the equations of motion for the coupled soil-structure system are given by eq.(16). Equation (16) may be rewritten in the following form where the correspondence of terms is self-evident.

$$\{\ddot{r}\} + [\bar{C}]\{\dot{r}\} + [\bar{K}]\{\dot{r}\} = -[\bar{\Gamma}]\{\ddot{u}\}_g \tag{18}$$

2.2 Soil Stiffness and Damping Properties

The matrices $[K_b]$ and $[C_b]$ of eq. (16) define the stiffness and damping characteristics of the supporting soil. The only restriction in the derivation to this point is the transformation of the dynamic characteristics of the soil to a point on the base mat. The matrices $[K_b]$ and $[C_b]$ may be derived from continuum theories or discrete models such as finite elements. The dynamic characteristics are, in general, frequency dependent. In the present study, the supporting soil is assumed to be uniform and adequately modeled by a linear elastic half-space. Further, it has been shown [2] that the frequency dependent characteristics of a linear elastic half-space may be adequately approximated by frequency independent characteristics. In this study, the frequency independent stiffness and damping values of Richart, Hall, and Woods [5] are utilized.

2.3 Direct Integration of the Equations of Motion

The basis for comparison of the results is the in-structure response spectra generated from a time-history analysis. The standard against which the subsequent analyses are measured is the numerical integration of eq. (18). The numerical technique applied is the Wilson theta method with the free parameter theta selected to be 1.4.

2.4 Modal Analysis

2.4.1 Uncoupled Equations of Motion

The coupled equations of motion of the soil-structure system, eq. (18), may be solved by numerical integration as mentioned previously. However, in many instances, it is desirable to perform a modal analysis. For example, the ability to perform a response spectrum analysis is dependent on uncoupling the equations of motion into modal coordinates. The soil-structure system, however, does not possess classical normal modes. The normal modes determined from the homogeneous undamped form of eq. (18) do not, in general, uncouple the damping matrix. Modal damping ratios denoted composite or equivalent modal damping ratios are determined by a technique such as one discussed herein.

The solution of the homogeneous undamped form of eq. (18) yields the eigenvectors $\{\psi_j\}$ and the undamped natural frequency $\bar{\omega}_j$ of the j^{th} mode of the soil-structure system. This leads to the equations of motion in modal coordinates:

$$\{\ddot{q}\} + [2\bar{\beta}_j\bar{\omega}_j]\{\dot{q}\} + [\bar{\omega}_j^2]\{q\} = -[\bar{\Gamma}]\{\ddot{u}\}_g \qquad (19)$$

where the quantity $\bar{\beta}_j$ is the unknown damping ratio of the jth mode.

2.4.2 Stiffness Proportional Composite Damping Ratios

One approach for determining the composite damping ratios is termed stiffness proportional composite damping. It corresponds to the hysteretic portion of the equivalent modal damping ratios computed by the technique of Roesset, Whitman, and Dobry [6]. The basic steps are to: associate a damping ratio with the stiffness of each member; construct a modified system stiffness matrix from the scaled element stiffnesses; and proportion the composite damping ratios according to the relative deformation of each member in each mode. The composite damping ratios are:

$$\bar{\beta}_j = \frac{<\psi_j>[\bar{K}]\{\psi_j\}}{<\psi_j>[K]\{\psi_j\}} \qquad (20)$$

where

$\bar{\beta}_j$ = composite modal damping ratio of the j^{th} mode;

$\{\psi_j\}$ = the mode shape vector for the j^{th} mode;

$[\bar{K}]$ = $\sum_{i=1}^{N}\beta_i\,[k_i]$, the modified stiffness matrix constructed from the product of the modal damping ratio and the stiffness matrix for each member;

N = the total number of members.

It has been common practice to limit the amount of damping associated with the soil to be 10% of critical viscous damping when utilizing stiffness proportional composite damping. This assumption is applied herein.

2.4.3 Composite Damping Ratios by Response Matching

A refined procedure for determining the composite damping ratios was developed by Tsai [2]. The technique is based on matching the steady-state response of the soil-structure system as determined by direct solution of eq.(18) and by modal analysis utilizing the modal coordinates of eq. (19). The system is excited at a series of natural frequencies corresponding to the frequencies $\bar{\omega}_j$ of the soil-structure system. Matching the response at a point within the soil-structure system leads to a series of nonlinear simultaneous equations in terms of the damping ratios. Their solution yields the composite damping ratios.

2.4.4 Composite Damping by Energy Proportioning

Another procedure for determining the composite damping ratios was presented by Roesset, Whitman, and Dobry [6]. In this approach, the composite damping ratios are comprised of two terms. One term accounts for energy assumed to dissipate in viscous form and the other term accounts for energy assumed to dissipate in a hysteretic form. The formula for the composite damping ratio of the j^{th} mode is:

$$\overline{\beta}_j = \frac{1}{2}\left(\frac{1}{\overline{\omega}_j} < \psi_j > [C_V] \{ \psi_j \} + \frac{1}{\overline{\omega}_j^2} < \psi_j > [C_H] \{ \psi_j \} \right) \quad (21)$$

where $[C_V]$ and $[C_H]$ are the viscous and hysteretic damping matrices, respectively. In the present study, the viscous portion is assumed to be made up of the horizontal and vertical components of the soil damping only. The remaining portion of the soil and super-structure damping is proportioned according to the hysteretic damping matrix.

3. Results

The results of this investigation are presented in the form of in-structure response spectra at selected locations in the RCB/PCRV configuration. Only data at the top of the PCRV, which is representative of the overall results and displays the largest differences in the methods, is presented herein. In Figs. 2-7, results generated by the analysis techniques of Section 2 are identified as follows. Method I refers to the numerical integration of eq. (18) and forms the basis for comparison of the other techniques. Methods II-IV identify the procedure for defining the composite damping ratios used in a time history modal analysis. Method II denotes the stiffness proportional composite damping approach. Method III is the technique of Tsai [2] discussed in Sec. 2.4.3. Method IV is the technique of Roesset, Whitman, and Dobry [6] discussed in Sec. 2.4.4. In Methods II and IV, a damping ratio for the soil is required. These damping ratios are defined in the manner suggested by Richart, Hall, and Woods [5], i.e., reducing the super-structure to a rigid disk of identical mass properties. As stated before, the soil damping ratios utilized in Method II are not permitted to exceed 0.10. The response spectra shown in Figs. 2-7 are for 2% of critical equipment damping.

Figures 2 and 3 present the design response spectra for the top of the PCRV in the horizontal and vertical directions, respectively. The design response spectra are formed by enveloping the design spectra for each individual site. The site spectra have been smoothed and the peaks spread by ± 15% prior to the enveloping process. The design response spectra for the horizontal direction are the same for Methods I-IV and shown as a solid curve in Fig. 2. In the vertical direction, the design response spectra are the same for Methods I, III, and IV and again shown as a solid curve in Fig. 3. The segmented curve of Fig. 3 represents the data generated by Method II which shows significant deviations from the other three techniques.

Figures 4-7 present raw response spectra at the top of the PCRV generated using the four techniques described herein. The data for two of the five sites, Sites 3 and 4, are displayed. Figures 4 and 5 show the results for the horizontal direction. Figures 6 and 7 show the results for the vertical direction. In both cases, Methods I, III, and IV produce results that are approximately the same. In the vertical direction, the differences between Methods I, III, and IV are not distinguishable. In both the horizontal and vertical directions, the significant deviations are due to Method II.

4. Conclusions

The results of this investigation led to separate conclusions concerning the applicability of the stiffness proportional composite damping method with a limited amount of soil damping (Method II) to the analysis of the soil-structure system depending on whether the response is in the horizontal or vertical direction. For the RCB/PCRV configuration examined herein, the different characteristics of the results in the horizontal and vertical directions are due to: (1) the coupling of the horizontal and rocking motions which is typical in many structures; and (2) the minor amount of amplification in the vertical direction through the structure itself. If design response spectra combining all site conditions are sought, the stiffness proportional composite damping method yields adequate results for the horizontal direction but overly conservative results in the vertical direction. The more refined techniques (Methods I, III, and IV) are preferred over the simplified method (Method II) whenever the individual results are desired.

5. References

[1] US NRC Regulatory Guide 1.60, "Design Response Spectra for Nuclear Power Plants," Revision 1.

[2] Tsai, N. C., "Modal Damping for Soil-Structure Interaction," J. Eng. Mech. Div., ASCE, Vol. 100, No. EM2, 323-341 (April 1974).

[3] Ibrahim, A. M., and Hadjian, A. H., "The Composite Damping Matrix for Three Dimensional Soil-Structure Systems, Proc. 2nd ASCE Specialty Conference on Structural Design of Nuclear Plant Facilities (December 1975) New Orleans.

[4] ASCE, Structural Analysis and Design of Nuclear Plant Facilities (Draft) (1976).

[5] Richart, F. E., Hall, J. R., and Woods, R. D., Vibrations of Soils and Foundations, Prentice-Hall, Englewood Cliffs, New Jersey (1970).

[6] Roesset, J. M., Whitman, R. V., and Dobry, R., "Modal Analysis for Structures with Foundation Interaction," J. Str. Div., ASCE, Vol. 99, No. ST3, 399-416 (March 1973).

Table I

Material Properties of Sites Considered

Material Property	Site 1 Competent Rock	Site 2 Soft Rock	Site 3 Firm Soil	Site 4 Intermediate Soil	Site 5 Soft Soil
V_p = Compressional Wave Velocity (feet/second)	15,000	7,285	4,000	2,700	1,000
V_s = Shear Wave Velocity (feet/second)	8,000	3,500	1,900	1,100	400
ν = Poisson's Ratio	0.3	0.35	0.35	0.4	0.4
ρ = Density (pounds/cubic foot)	180	130	115	100	100
E = Young's Modulus (pounds/square inch)	6.5×10^6	9.45×10^5	2.43×10^5	7.0×10^4	1.01×10^4
G = Shear Modulus (pounds/square inch)	2.5×10^6	3.5×10^5	9.0×10^4	2.5×10^4	3.6×10^3

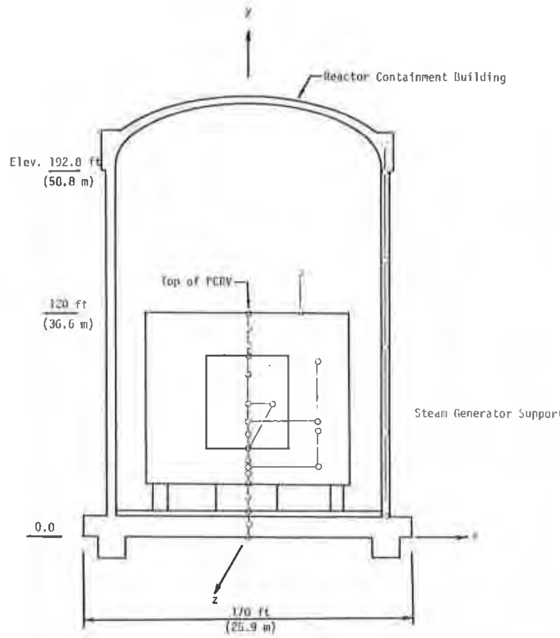

1. HTGR Reactor Containment Building/Prestressed Concrete Reactor Vessel with Mass Point Locations.

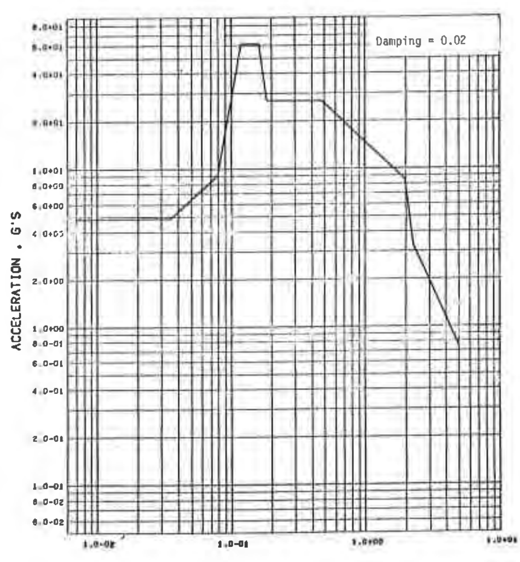

2. In-Structure Design Response Spectra - Top of PCRV - Horizontal Direction - 1.0 G OBE

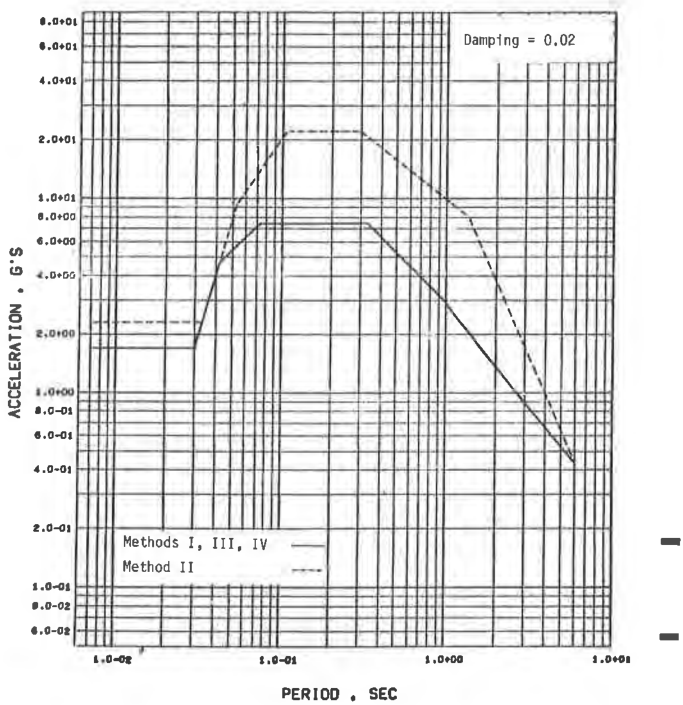

3. In-Structure Design Response Spectra - Top of PCRV - Vertical Direction - 1.0 G OBE

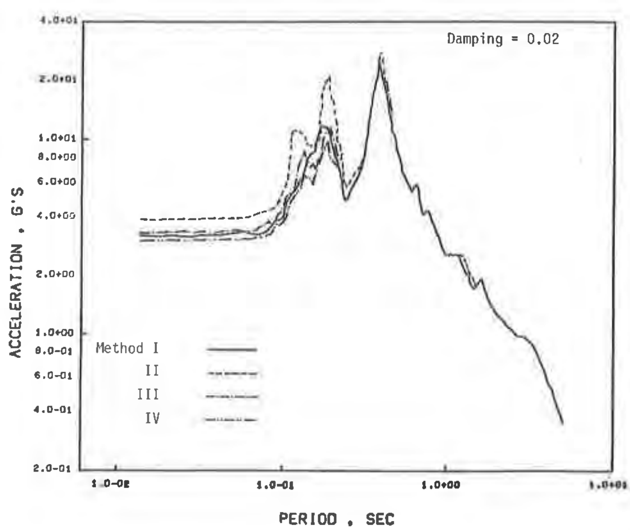

4. In-Structure Response Spectra - Top of PCRV - Horizontal Direction - Site 3 - 1.0 G OBE

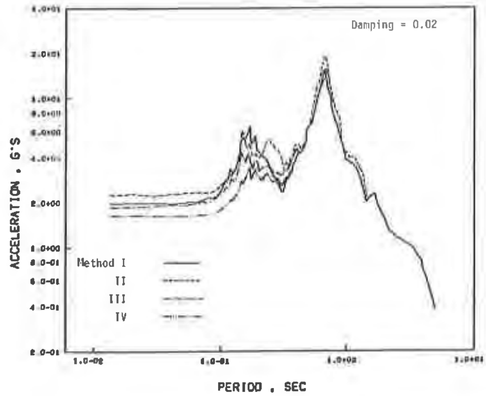

5. In-Structure Response Spectra - Top of PCRV - Horizontal Direction - Site 4 - 1.0 G OBE

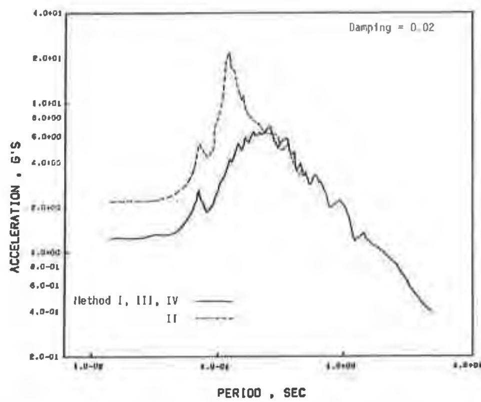

6. In-Structure Response Spectra - Top of PCRV - Vertical Direction - Site 3 - 1.0 G OBE

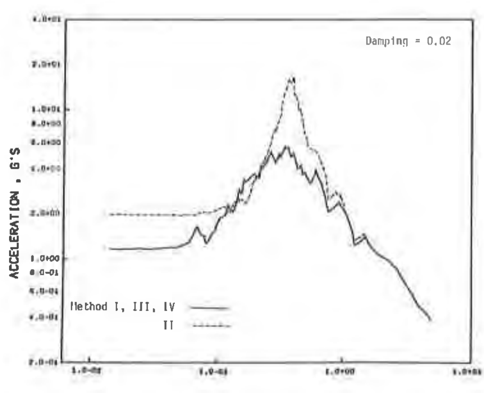

7. In-Structure Response Spectra - Top of PCRV - Vertical Direction - Site 4 - 1.0 G OBE